

Parametric optimization of system parameters and characteristics of solar air heater with different geometries.

Mayank Mani Pandey¹, Rahul Bahuguna²

¹ Faculty of Technology, Uttarakhand Technical University Dehradun, Uttarakhand, India

² Asst. Professor, Dept. of Mechanical Engineering, Faculty of Technology, Uttarakhand Technical University Dehradun,

Abstract - The scope of this study deals with the parametric optimization of the system parameters based on effective efficiency criterion of the impingement jets of the various geometries. The optimum values required of the system parameters will be useful to determine the geometrical set of parameters which delivers the higher Nusselt Number and lower Friction Factor.

Key Words: Heat transfer coefficient; jet impingement; Nusselt number; Reynolds number; thermal efficiency; effective efficiency.

1. INTRODUCTION

The thermal efficiency of a solar air heater is significantly low because of low convective heat transfer coefficient between the absorber plate and air, leading to high absorber plate temperature and greater amount of heat losses to the ambient. It has been found that the main thermal resistance to the convective heat transfer is due to the formation of boundary layer on the heat transferring surface. Efforts for enhancing heat transfer have been directed towards artificially destroying or disturbing this boundary layer.

1.1 Improvement of heat transfer from the absorber plate

The thermal efficiency of a solar air heater is generally low because of low heat transfer coefficient between absorber plate and air flowing in the duct, which leads to higher absorber plate temperature, thus higher thermal losses. By lowering the temperature of the absorber plate these thermal losses can be reduced which enhances the rate of heat transfer between absorber plate and air. The thermal losses can be reduced by using:

- Extended surface on the absorber plate
- Porous material in the air flow duct
- Turbulence promoters

1.2 Artificial Roughness

The artificial roughness in the form of repeated ribs is one of the effective and economic ways of improving the performance of a solar air heater. Ribs break the viscous sub layer and create local wall turbulence due to separation and reattachment of flow without disturbing the core turbulent flow resulting in improvement of convective heat transfer coefficient between air and the absorber plate. The application of artificial roughness in the form of fine wires or ribs of different geometry on the heat transfer surface has been recommended to increase the heat transfer coefficient by several investigators.

Several different types and shapes of geometries of artificial roughness have been proposed and investigated. The types include transverse, inclined, v-shaped, rib-grooved, ribs with gaps, discrete or continuous, multiple-v ribs, v with gap, chamfered, wedge shaped ribs, dimpled, expanded metal mesh, arc-shaped ribs etc. It has been found that each shape is represented by sets of geometrical dimensionless parameters that characterize the geometry. Such parameters include relative roughness height, relative roughness pitch, angle of attack, relative groove position, relative gap width, relative gap position etc.

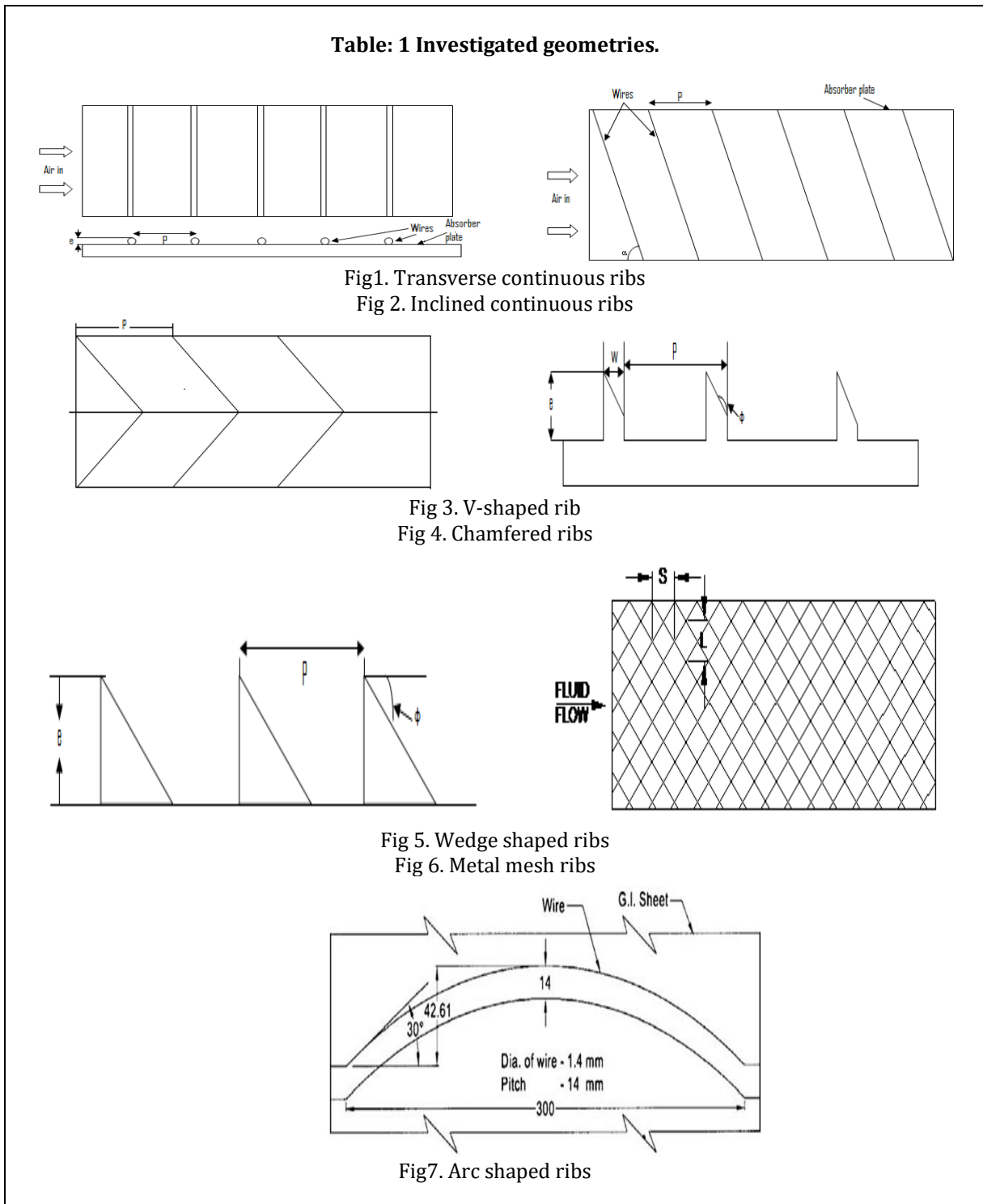
Several investigators have experimentally investigated the heat transfer and fluid flow characteristics of these different geometries and developed correlations for Nusselt number and friction factor as a function of geometrical parameters. They have also discussed the relative enhancement in Nusselt number achieved by the use of artificial roughness.

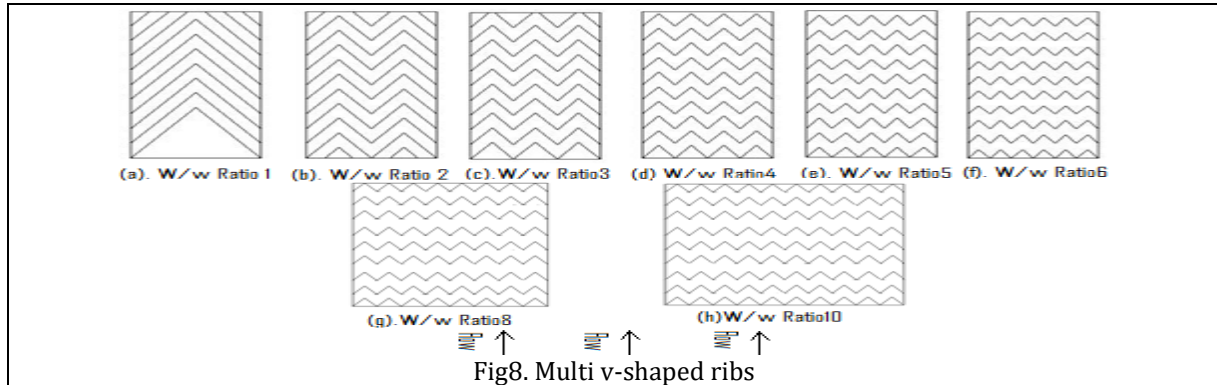
The performance of solar air heaters as a result of the use of artificial roughness on the underside of absorber plate of solar air heater has been investigated and the enhancement in thermal efficiency as a function of roughness parameters has been presented and discussed.

However, it is pointed out that an enhancement in heat transfer and hence thermal performance is accompanied by substantial increase in friction factor and hence pressure losses and energy expenditure to make the air flow through the

collector. Thus there is need to consider both enhancement of thermal performance of collector and the additional friction energy expenditure simultaneously i.e. by thermo-hydraulic consideration. Thermo hydraulic optimization has been carried out by several investigation and optimum values of roughness parameters have been obtained for different roughness geometries.

Various aspects of the investigations including experimentation on heat transfer and fluid flow characteristics of different types of geometries and other methods of analysis, thermal and thermo hydraulic performance and optimization are shown below.





1.3 Jet Impingement

High speed jet impingement on a surface creates a thin boundary layer and gives an enhanced heat transfer. The experimental geometrical parameters are relative height ratio (e_d / P_p) from 0.5 to 2.0, relative width ratio (W_w / P_{AP}) from 1.0 to 6.0, angle of arc (α_a) from 35° to 75° , relative pitch ratio (P_p / e_p) from 8.0 to 12. The flow Reynolds number varied from 5000 to 19,000. The maximum enhancement is achieved at W_w / P_{AP} 5.0, $e_p / d_p = 1.0$, $P_p / e_p = 9.5$ and $\alpha_a = 55^\circ$. The correlation for Nusselt number and friction factor was developed as:

$$Nu = 0.0476 Re^{1.0119} W_A / W_{AP}^{0.4228} \exp[0.0529(\ln(W_A / W_{AP}))^2] (e_p / d_p)^{-0.133} \exp[-0.228(\ln(e_p / d_p))^2] (P_p / e_p)^{-0.1455} \exp(-0.3069(\ln(P_p / e_p))^2) (\alpha / 55)^{-0.7522} \exp(-1.4876(\ln(\alpha / 60))^2)$$

$$f = 15.601 Re^{-0.1434} W_A / W_{AP}^{0.2569} \exp[0.1205(\ln(W_A / W_{AP}))^2] (e_p / d_p)^{-0.1708} \exp[-0.3957(\ln(e_p / d_p))^2] (P_p / e_p)^{-0.2777} \exp(-0.5793(\ln(P_p / e_p))^2) (\alpha / 55)^{-0.9011} \exp(-1.7618(\ln(\alpha / 60))^2)$$

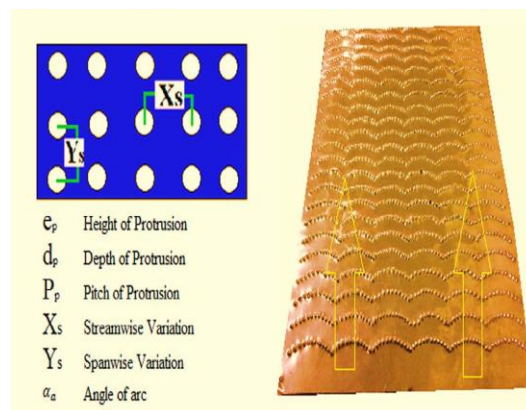


Fig. 9. Multiple arc jet impingement.

2. PROBLEM FORMULATION:

After conducting a comprehensive literature review, it has been observed that very few investigations examined the parametric optimization of the geometrical parameters selected for investigation. The present work deals with the parametric optimization of the system parameters based on effective efficiency criterion of impingement jets solar air heater with multiple protrusion arc obstacles. The optimum values of the system parameters will be useful to determine the geometrical set of parameters which delivers the higher Nusselt Number and lower friction factor. The parameters selected for investigation are listed in Table 1.

Table 1: Range of experimental parameters

Sr.No.	Parameters	Symbol	Range
1.	Relative width ratios	(W_P/W_{AP})	1.0 - 6.0
2.	Relative height ratios	(e_P/d_P)	0.5 - 2.0
3.	Relative pitch ratios	(P_P/e_P)	8.0 - 12
4.	Angle of arc	(α_a)	35° - 75°
5.	Reynolds Number	(Re)	5000 - 19000

Accordingly, it is proposed to carry out the investigation on the parametric optimization of the system parameters to determine the optimum set that delivers higher heat transfer with nominal pressure drop penalty.

2.1. METHODOLOGY

The following two criteria have been proposed to be considered for the optimization of roughness parameters of artificially roughened solar air heaters.

Thermal Efficiency, η_{th}

Effective efficiency, η_{eff}

A brief explanation of each of this criterion is given below:

Thermal Efficiency (η_{th})

$$\eta = \frac{Q_u}{IA_c} \quad (6.1)$$

Effective Efficiency (η_{eff})

$$\eta_{eff} = \frac{(Q_u - \frac{P_m}{C})}{IA_p} \quad (6.2)$$

where 'C' is the conversion factor to account for the conversion of thermal energy to mechanical energy and is given by:

$$C = \eta_F \eta_m \eta_{tr} \eta_{th}$$

where,

η_F is the efficiency of the fan

η_m is the efficiency of the electric motor

η_{tr} is the efficiency of electrical transmission from the power plant

η_{th} is the efficiency of thermal conversion of the power plant.

The value of 'C' as recommended by Corter and Piacentini [1990] is 0.18 (typical value of efficiency factors being:

$\eta_F=0.65$, $\eta_m=0.88$, $\eta_{tr}=0.925$ and $\eta_{th}=0.344$).

3. CONCLUSIONS

It may be noted that since the objective of this work is to present a methodology for optimal design of the solar air heater, the results need to be presented as function of two basic design parameters namely,

Temperature rise parameter, $\Delta T/I$ (ratio of air temperature rise, ΔT , across the collector to the average intensity of solar insolation, I) and Solar insolation (I)

The calculation starts with fixed value of these parameters ($\Delta T/I$ and I) and proceeds with the calculation of the other parameters for a given collector. Step by step procedure of calculation is given below:

It is pointed out here that the steps 1 to step 18 are the same as stated in the previous chapter. However these have reproduced here for the purpose of completeness.

Step 1. A set of the values of the roughness parameters namely number of gaps (N_g), relative gap width (g/e), angle of attack (α) and relative roughness pitch (P/e) is selected for which the calculation is to be performed.

Step 2. A set of values of design parameters namely temperature rise parameter, ($\Delta T/I$) solar insolation, I is selected.

Step 3. Area of plate is calculated as,

$$A_p = W \times L \quad (6.6)$$

Step 4. Hydraulic diameter of duct is calculated as;

$$D = \frac{2(W \times H)}{W + H} \quad (6.7)$$

Step 5. Fixed system parameters such as;

Thermal conductivity of insulation, k_i

Thickness of insulation, t_i

Transmittance-absorptance product, ($\tau\alpha$)

Emissivity of the absorber plate, ε_p

Emissivity of the glass covers, ε_g

Fixed operating parameters such as;

Atmospheric air velocity (V_w) and atmospheric temperature (T_a) are selected.

Step 6. The temperature rise ΔT of air and outlet temperature T_o is calculated as,

$$\Delta T = \frac{\Delta T}{I} \times I \quad (6.8)$$

$$T_o = \Delta T + T_i \quad (6.9)$$

Step 7. Approximate initial mean plate temperature is assumed as;

$$T_p = \frac{T_o + T_i}{2} + 10^\circ\text{C} \quad (6.10)$$

Step 8. Using the value of the plate temperature T_p , value of top loss coefficient, U_t is computed by using equation proposed by Klein [1953] given as,

$$U_t^{-1} = \left[\frac{\sigma(T_p^2 + T_g^2)(T_p + T_g)}{\left(\frac{1}{\varepsilon_p} + \frac{1}{\varepsilon_g} - 1\right)} + \left(\frac{k_a \text{Nu}}{L_g}\right) \right]^{-1} + [\sigma\varepsilon_g(T_p^2 + T_g^2)(T_p + T_g) + h_w]^{-1} + \frac{t_g}{k_g} \quad (6.11)$$

where

$$T_g = \left(\frac{F_1 T_p + c T_a}{1 + F_1} \right)$$

where,

$$F_1 = \frac{[12 \times 10^{-8}(T_a + 0.2T_p)^3 + h_w]^{-1} + 0.3t_g}{[6 \times 10^{-8}(\epsilon_p + 0.028)(T_p + 0.5T_a)^3 + 0.6L_g^{-0.2}\{(T_p - T_a)\cos\beta\}^{0.25}]^{-1}}$$

and

$$c = \left(\frac{(T_s/T_a) + (h_w/3.5)}{(1 + (h_w/3.5))} \right)$$

$$T_s = 0.0522(T_a)^{1.5}$$

$$Nu = 1 + 1.44[1 - 1708/Ra \cos\beta]^+ \{1 - 1708(\sin 1.8\beta)^{1.6}/Ra \cos\beta\} + [(Ra \cos\beta/5830)^{0.33} - 1]$$

where, $Ra = Gr \times Pr$

$$Gr = \frac{g\beta'(T_p - T_g)L_g^3}{\nu^2}$$

$$\beta' = \frac{1}{[(T_o + T_i)/2]}$$

$$Pr = \frac{\mu \cdot C_p}{k_a}$$

Back loss coefficient U_b is expressed as;

$$U_b = k_i/t_i$$

The edge loss coefficient, based on the collector area A_p is given as;

$$U_e = \frac{(L + W)t_e k_i}{LWt_i}$$

finally,

$$U_L = U_t + U_b + U_e \quad (6.12)$$

Step 9. Useful energy gain is calculated as;

$$Q_{u1} = [I(\tau\alpha) - U_L(T_p - T_a)]A_p \quad (6.13)$$

Step 10. Mass flow rate is determined from the expression given as;

$$m = \frac{Q_{u1}}{C_p \Delta T} \quad (6.14)$$

Step 11. Reynolds number of flow of air in the duct is computed as;

$$Re = \frac{GD}{\mu} \quad (6.15)$$

where, G is the mass velocity of air through the collector

$$G = \frac{m}{WH} \quad (6.16)$$

Step 12. The Nusselt number (Nu) is calculated using the correlation developed in previous chapter, which is reproduced below,

$$Nu = 0.0476 Re^{1.0119} W_A/W_{AP}^{0.4228} \exp[0.0529(\ln(W_A/W_{AP}))^2] (e_p/d_p)^{-0.133} \exp[-0.228(\ln(e_p/d_p))^2] (P_p/e_p)^{-0.1455} \exp(-0.3069(\ln(P_p/e_p)))^2 (\alpha/55)^{-0.7522} \exp(-1.4876(\ln(\alpha/60)))^2 \quad (6.17)$$

Step 13. The convective heat transfer coefficient is calculated as follows,

$$h = \frac{\text{Nu} \cdot k}{D} \quad (6.18)$$

The plate efficiency factor is then determined as,

$$F' = \frac{h}{h + U_L} \quad (6.19)$$

Step 14. The heat removal factor is calculated as,

$$F_o = \frac{mC_p}{A_p U_L} \left[\exp \left\{ \frac{F' U_L A_p}{mC_p} \right\} - 1 \right] \quad (6.20)$$

Step 15. The useful heat gain, Q_{u2} is computed as,

$$Q_{u2} = F_o A_p [I(\tau\alpha) - U_L (T_o - T_i)] \quad (6.21)$$

Step 16. At this stage, the difference between the two values of useful heat gain Q_{u1} and Q_{u2} is checked. Ideally the two values should be same. However, if the difference in two values is more than 0.1% of Q_{u1} , then the plate temperature is modified as,

$$T_p = T_a + \left[\frac{I(\tau\alpha) - \frac{Q_{u2}}{A_p}}{U_L} \right] \quad (6.22)$$

Step 17. Using the new plate temperature, the calculations from step 6 to 20 are performed again till the difference between the two values of useful heat gain, Q_{u1} and Q_{u2} is reduced to a value below 0.1% of Q_{u1} .

Step 18. Friction factor, f is calculated using the correlation developed in a previous chapter, which is reproduced below:

$$f = 15.601 \text{Re}^{-0.1434} W_A / W_{AP}^{0.2569} \exp \left[0.1205 (\ln(W_A / W_{AP}))^2 \right] (e_p / d_p)^{-0.1708} \exp \left[-0.3957 (\ln(e_p / d_p))^2 \right] (P_p / e_p)^{-0.2777} \exp(-0.5793 (\ln(P_p / e_p)))^2 (\alpha / 55)^{-0.9011} \exp(-1.7618 (\ln(\alpha / 60)))^2 \quad (6.23)$$

Step 19. Using the value of friction factor, the pressure drop $(\Delta P)_d$, across the duct is calculated as follow:

$$(\Delta P)_d = \frac{4fL\rho V^2}{2D} \quad (6.24)$$

Step 20. Using the value of $(\Delta P)_d$, the mechanical power (P_m) is calculated as,

$$P_m = \frac{m(\Delta P)_d}{\rho} \quad (6.25)$$

Step 21. Thermal efficiency is calculated as;

$$\eta_{th} = F_o \left[(\tau\alpha) - \frac{U_L(T_o - T_i)}{I} \right] \quad (6.26)$$

Step 22. The effective efficiency, η_{eff} , is calculated as;

$$\eta_{eff} = \frac{Q_u - \left(\frac{P_m}{C}\right)}{I \cdot A_p} \quad (6.27)$$

Step 23. Logarithmic mean fluid temperature (T_{fm}) is calculated as follow,

$$T_{fm} = \frac{T_o - T_i}{\ln\left(\frac{T_o}{T_i}\right)} \quad (6.28)$$

Step 24. Carnot efficiency based on logarithmic mean fluid temperature as source and ambient temperature as sink can be calculated as follows,

$$\eta_c = 1 - \left(\frac{T_i}{T_{fm}}\right) \quad (6.29)$$

Step 25. Net exergy flow is calculated as

$$E_n = IA_p \eta_{th} \eta_c - P_m (1 - \eta_c) \quad (6.30)$$

Step 26. Exergy input is calculated as;

$$E_s = I \left(1 - \frac{T_a}{T_{sun}}\right) \quad (6.31)$$

Step 27. Exergetic efficiency is calculated as;

$$\eta_{exg} = \frac{E_n}{E_s} \quad (6.32)$$

Step 28. The next set of values of temperature rise parameter and insolation is then selected and the calculations from steps 3 to 29 are repeated, to cover the entire range of values of temperature rise parameter and insolation.

Step 29. The next set of values of roughness parameters namely, number of gaps (N_g), relative gap width (g/e), angle of attack (α) and relative roughness pitch (P/e) are then selected and the calculation from steps 2 to 30 are repeated, to cover the entire range of values of roughness parameters.

Based on these considerations, optimization in terms of geometrical parameters of roughness elements as function of operating parameters will be carried out. These results will be helpful to be used for optimal design of roughness geometry.

REFERENCES

- [1] Goswami, D.Y., Vijayraghvan, S., Lu, S. and Tamm, G., 2004, New and emerging developments in solar energy, Solar Energy, Vol. 76, pp. 33-43.
- [2] Duffie, J.A. and Beckman, W.A., 1991, Solar engineering of thermal processes", John Wiley and Sons, New York.

- [3] Aharwal K R, Gandhi B K, Saini J S., 2008, Experimental investigation on heat-transfer enhancement due to a gap in an inclined continuous rib arrangement in a rectangular duct of solar air heater. *Renew Energy*, 33:585–96.
- [4] Chamoli Sunil, Thakur NS, Saini JS., 2012, A review of turbulence promoters used in solar thermal systems. *Renewable and Sustainable Energy Reviews* 16, 3154– 3175.
- [5] Prasad, B.N. and Saini, J.S., 1988, Effect of artificial roughness on heat transfer and friction factor in a solar air heater, *Solar Energy*, Vol. 41, No. 6, 555-560.
- [6] Gupta D, Solanki SC, Saini JS., 1993, Heat and fluid flow in rectangular solar air heater ducts having transverse rib roughness on absorber plates. *Sol Energy*, 51(1):31–7.
- [7] Hans V.S., 2009, Heat transfer and friction characteristics of multi v-rib roughened solar air heater, Ph.D Thesis Deptt of AHEC IIT Roorkee(India).